

# Control of the damage threshold of Si via a SiO<sub>2</sub> coating upon irradiation with Mid-IR femtosecond laser pulses

G. D. Tsibidis <sup>1\*</sup> and E. Stratakis <sup>1,2\*</sup>

<sup>1</sup> *Institute of Electronic Structure and Laser (IESL), Foundation for Research and Technology (FORTH), N. Plastira 100, Vassilika Vouton, 70013, Heraklion, Crete, Greece*

<sup>2</sup> *Department of Physics, University of Crete, 71003 Heraklion, Greece*

A key issue in the use of high-power mid-infrared (Mid-IR) laser sources for a plethora of applications is the investigation of the exciting laser driven physical phenomena taking place in materials coated with dielectric films. Here, we present a theoretical investigation of the ultrafast processes and thermal response upon excitation of two-layered complexes consisting of fused silica thin films placed on silicon substrates with ultrashort pulsed lasers in the Mid-IR spectral regime. Through the development of a theoretical model, we demonstrate that the control of the underlying ultrafast phenomena and the damage threshold (DT) of the substrate are achieved via an appropriate modulation of the thickness of the SiO<sub>2</sub> film. It is shown that a decrease of DT by up to 27% compared to the absence of coating is feasible emphasising the impact of coatings of a lower refractive index than the substrate. Besides this, it is demonstrated that no absorption of energy occurs within the SiO<sub>2</sub> layer, therefore the dynamics of the reflectivity of the two-layered complex is directly associated with the electron excitation in the substrate. These remarkable predictions can be employed for the development of new optical coatings and components for nonlinear optics and photonics for a large range of Mid-IR laser-based applications.

## I. INTRODUCTION

Irradiation of semiconducting materials (i.e. Silicon, Germanium, etc.) with high intensity femtosecond (fs) laser beams in the Mid-IR spectral region raises challenging opportunities in photonics and an abundance of applications [1-5] due to the exciting laser driven phenomena compared with pulses at lower wavelengths [6-8]. The pronounced transparency of the semiconductors at Mid-IR compared to their behaviour at the visible and near-infrared regimes (i.e. leading to a noticeable absorption dynamics [6-8]), the excitation of electromagnetic modes such as surface plasmon (i.e. crucial for laser machining purposes [9] and for functioning of the material as a novel plasmonic tool [4, 5, 10]) at lower excitation levels, and the expected influence of the electron excitation/plasma formation through the scaling of the ponderomotive energy  $U_p$  with the laser wavelength (i.e.  $U_p \sim \lambda_L^2$  where  $\lambda_L$  stands for the laser wavelength) constitute some physical phenomena which are characteristic of the Mid-IR spectral region [3].

It is evident that a precise knowledge of the fundamentals of laser interaction with the target material and the elucidation of the aforementioned phenomena in various laser conditions are very crucial for the efficient employment of the Mid-IR based technology in various applications. In particular, a key technological and fundamental challenge in the research of how materials respond upon exposure to Mid-IR fs pulses is relevant to the determination of the damage threshold (DT) of the target which is defined as the smallest fluence that induces minimal damage on the surface of the irradiated solid. In previous reports, DT measurements (through appropriate experimental protocols [11, 12]) and predictions (via the development of theoretical models [9, 11]) were presented in various laser conditions and laser wavelengths for Silicon and it has been deduced that understanding of the fundamentals of the strong field interaction with Silicon (Si) [9, 13] /Germanium (Ge) [14] in the Mid-IR regime can lead to efficient laser-based patterning.

Nevertheless, despite the interesting physical phenomena produced on bulk semiconductors irradiated with strong laser fields, there still exist fundamental open questions in regard to the effects on two-layered semiconducting/dielectric materials. More specifically, it is evident that a lack of knowledge of how coated materials respond to Mid-IR pulses and how DT scales with  $\lambda_L$  prevents the optimization of the use of pulses in this regime for technological applications. Given the transparency of low- and high- bandgap materials in the Mid-IR regime, Si, ZnS, Ge as well as fluorides and fused Silica (SiO<sub>2</sub>) have been used as high-performance coatings for Mid-IR related applications [15, 16]. In a recent report [17], it was shown that the employment of Si films as a coating on top of SiO<sub>2</sub> increases the damage threshold of the bulk substrate and this behaviour is dependent on the thickness of Si. Furthermore, the optical parameters of the two-layered material can also be modulated via an appropriate selection of the coating thickness. Interestingly, despite Si is a lower band-gap material than SiO<sub>2</sub>, the Si film does not absorb any amount of the laser energy deposited in the complex.

On the other hand, a key issue in the manufacturing of optical components providing the optothermal response of Si at long wavelengths, is whether a two-layered complex consisting of a coating (i.e. transparent in Mid-IR) of lower refractive index than that of the semiconductor on top of bulk Si leads to a variation of DT of the substrate. Fused silica represents a well-characterised material and a fundamental question is pertinent to whether SiO<sub>2</sub> coatings of various thicknesses could result in a different optical and thermal response of the Si substrate upon irradiation with Mid-IR fs pulses. Thus, the evaluation of how a SiO<sub>2</sub>/Si complex behaves can potentially lead to an increase of the throughput of

the system, allow a control of the DT of the substrate and enable the reduction of undesired effects generated by reflections; however, such an assessment requires unraveling the ultrafast phenomena that take place during irradiation of SiO<sub>2</sub>/Si with strong Mid-IR fs pulses. The elucidation of the aforementioned issues is of paramount importance not only to understand further the underlying physical processes of laser-matter interactions and ultrafast electron dynamics but also to associate the induced thermal effects with damage on the substrate. To this end, a systematic exploration of the correlation of the laser parameters (i.e. fluence, pulse duration, wavelength) and material features (i.e. thickness of film) with the resulting effects on the surface of the substrate are aimed to potentially create novel capabilities for material processing.

Motivated by the above challenges, in the current work, a detailed theoretical investigation is conducted aiming to correlate the ultrafast dynamics, thermal effects and damage threshold on the Silicon substrate in various laser conditions and SiO<sub>2</sub> coating thicknesses; in particular, a thermal criterion is assumed for DT (i.e. material reaches the melting temperature). The paper is organised as follows: in Section II, a detailed theoretical framework is presented to describe the physical mechanisms that account for the ultrafast dynamics and thermal effects upon irradiation of SiO<sub>2</sub>/Si with Mid-IR fs laser pulses in various laser conditions and thicknesses of the SiO<sub>2</sub> coating. The model not only takes into account a dynamic variation of the optical and thermophysical properties but also, the influence of the optical coating thickness on the response of the material is also discussed. A systematic analysis of the results is illustrated in Section III while concluding remarks follow in Section IV.

## II. THEORETICAL MODEL

A key role in the elucidation of the effects that lead to material damage is the energy absorption from the two-layered material; in particular, the composition of the complex, structural characteristics (i.e. thickness of the materials) are aimed to tailor the optical parameters and, therefore, determine the amount of absorbed energy. Thus, a crucial investigation requires the evaluation of the optical properties of SiO<sub>2</sub>/Si structures for various thicknesses  $d$  of the coating. In Fig.1, the two-layered complex, SiO<sub>2</sub>/Si (a SiO<sub>2</sub> film of thickness  $d$  on top of a bulk Si is considered), irradiated with mid-IR pulses is sketched.

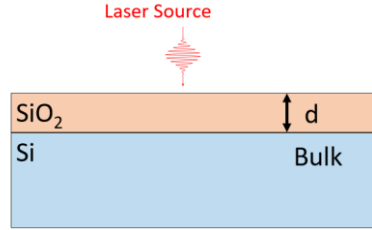


Figure 1: A two-layered complex (a SiO<sub>2</sub> film of thickness  $d$  on top of bulk Si irradiated with a mid-IR laser pulse).

The calculation of the reflectivity  $R$ , transmissivity  $T$  and the absorbance  $1-R-T$  in the upper layer are derived via the employment of the multiple reflection theory [18]. More specifically, the following expressions are employed to evaluate the optical parameters for a thin film placed on a thick substrate assuming a  $p$ -polarised beam although other polarization states can also be included (at room temperature [18, 19])

$$R = |r_{dl}|^2, \quad T = |t_{dl}|^2 \tilde{N}_S, \quad r_{dl} = \frac{r_{am} + r_{ms} e^{2\beta j}}{1 + r_{am} r_{ms} e^{2\beta j}},$$

$$t_{dl} = \frac{t_{am} t_{ms} e^{\beta j}}{1 + r_{am} r_{ms} e^{2\beta j}}, \quad \beta = 2\pi d \tilde{N}_m / \lambda_L \quad (1)$$

$$r_{am} = \frac{\tilde{N}_m - \tilde{N}_a}{\tilde{N}_m + \tilde{N}_a}, \quad r_{ms} = \frac{\tilde{N}_S - \tilde{N}_m}{\tilde{N}_S + \tilde{N}_m}, \quad t_{am} = \frac{2\tilde{N}_a}{\tilde{N}_m + \tilde{N}_a}, \quad t_{ms} = \frac{2\tilde{N}_m}{\tilde{N}_S + \tilde{N}_m}$$

where the indices 'a', 'm', 'S' stand for 'air', 'SiO<sub>2</sub>', 'Si', respectively. The refractive indices of the materials such as air, Si and SiO<sub>2</sub> are equal to  $\tilde{N}_a = 1, \tilde{N}_S, \tilde{N}_m$ , respectively at the laser wavelength  $\lambda_L$ .

Following the precise evaluation of the energy absorbed from the SiO<sub>2</sub>/Si complex, the next module of the theoretical model is related to the description of electron excitation and relaxation processes in the SiO<sub>2</sub> and Si materials.

### a. Ultrafast dynamics in SiO<sub>2</sub>

To describe the free electron generation in SiO<sub>2</sub> upon excitation with ultrashort Mid-IR pulsed lasers a standard

model of two rate-equations (Eq.2) is used; these single rate-equations yield both the evolution of the excited electron and self-trapped exciton (STE) densities,  $N_e$  and  $N_{STE}$  [20, 21], respectively,

$$\begin{aligned}\frac{dN_e}{dt} &= \frac{N_V - N_e}{N_V} (W_{PI}^{(1)} + N_e A^{(1)}) + \frac{N_{STE}}{N_V} (W_{PI}^{(2)} + N_e A^{(2)}) - \frac{N_e}{\tau_{tr}} \\ \frac{dN_{STE}}{dt} &= \frac{N_e}{\tau_{tr}} - \frac{N_{STE}}{N_V} (W_{PI}^{(2)} + N_e A^{(2)})\end{aligned}\quad (2)$$

where  $N_V = 2.2 \times 10^{22} \text{ cm}^{-3}$  stands for the valence electron density. In Eqs.2, the STE states are considered to be centres situated at an energy level below the conduction band (i.e.  $E_G^{(2)} = 6 \text{ eV}$ ); it is recalled that, for  $\text{SiO}_2$ , the band gap between the valence (VB) and the conduction band (CB) is  $E_G^{(1)} = 9 \text{ eV}$  [20, 22] while  $\tau_r \sim 150 \text{ fs}$  [23] stands for the trapping time of electrons in STE states. In the above framework, photoexcitation assumes photoionization ( $W_{PI}^{(i)}$ , which can be due to multiphoton, tunneling or multiphoton/tunneling ionization) and impact ionization processes (i.e.  $A^{(i)}$  stands for the avalanche ionisation rate) which can allow a transition from VB to CB ( $i=1$ ) and from STE level to CB ( $i=2$ ). As shown in previous reports [23-25], the electron excitation mechanisms are dependent on the laser intensity  $I$ . In the present model, an attenuation of the local laser intensity due to the photoionisation and inverse bremsstrahlung (Free Carrier) absorption along the depth  $z$  of the dielectric is considered and described by Eq.3

$$\begin{aligned}\frac{dI}{dz} &= N_{ph}^{(1)} \hbar \omega_L \frac{N_V - N_e}{N_V} W_{PI}^{(1)} + N_{ph}^{(2)} \hbar \omega_L \frac{N_{STE}}{N_V} W_{PI}^{(2)} - \alpha(N_e) I \\ I &= (1 - R - T) \frac{2\sqrt{\ln 2}}{\sqrt{\pi} \tau_p} F e^{-4 \ln 2 \left( \frac{t - 3\tau_p}{\tau_p} \right)^2}\end{aligned}\quad (3)$$

where  $N_{ph}^{(i)}$  stands for the minimum number of photons required to be absorbed by an electron located in the valence band ( $i=1$ ) or the band where the STE states reside ( $i=2$ ) to overcome the relevant energy gap and reach the conduction band. For the sake of simplicity, films of thicknesses which are remarkably smaller than the size of the spot radius of the laser beam are considered that allows to model the multiscale processes in one dimension (along the  $z$ -axis). On the other hand,  $F$  and  $\omega_L$  correspond to the laser fluence and frequency while  $1 - R - T$  stands for the absorptivity of the dielectric material. Finally, the last term in the first equation in Eq.3 corresponds to inverse bremsstrahlung while the carrier density dependent parameter  $\alpha$  corresponds to the free carrier absorption coefficient.

## b. Ultrafast dynamics in Si

On the other hand, the ultrafast dynamics in Si is described by the following set of equations (Eq.4)

$$\begin{aligned}\frac{dN_e^{(Si)}}{dt} &= \frac{\beta_{TPA}}{2\hbar\omega_L} I^2 + \frac{\gamma_{TPA}}{3\hbar\omega_L} I^3 - \gamma(N_e^{(Si)})^3 + \theta N_e^{(Si)} - \vec{\nabla} \cdot \vec{J} \\ \frac{dI}{dz} &= -\alpha_{FCA} I - \beta_{TPA} I^2 - \gamma_{TPA} I^3 \\ I &= T \frac{2\sqrt{\ln 2}}{\sqrt{\pi} \tau_p} F e^{-4 \ln 2 \left( \frac{t - 3\tau_p}{\tau_p} \right)^2}\end{aligned}\quad (4)$$

In the above expressions,  $\beta_{TPA}$ ,  $\gamma_{TPA}$ ,  $\alpha_{FCA}$  stand for the two-photon, three-photon and free carrier absorption, respectively,  $\vec{J}$  is the carrier current density (see below) and  $T$  corresponds to the transmissivity that is also related to the absorbed part of the laser intensity from the substrate. Furthermore,  $N_e^{(Si)}$  correspond to the carrier density inside Si while  $\theta$  stands for the impact ionisation coefficient. For a more detailed description of the ultrafast dynamics for Si, see Ref. [9]. It is noted that, in this work, the multiphoton ionisation process considers only two-photon and three-photon absorption processes as the focus was centred on laser wavelengths between  $2.2 \mu\text{m}$  and  $3.2 \mu\text{m}$ , where two-photon and three-photon excitation dominates the multiphoton excitation mechanism [9, 26-29]. An extension of the model at longer wavelengths (i.e. smaller photon energies) requires the knowledge of higher order absorption coefficient.

It is known that the optical parameters of a material vary with the excitation level reached during the irradiation [30, 31] which implies that a precise evaluation of the ultrafast phenomena requires the calculation of the dynamics of reflectivity, transmissivity and absorptivity. The calculation of the optical parameters is performed through the evaluation of the dielectric function  $\epsilon$ , which is related to the refractive index  $n$  and extinction coefficient  $k$  through the expression  $\epsilon = (n + ik)^2$ . It is recalled that the refractive indices  $n$  of *unexcited* Si and  $\text{SiO}_2$  in Mid-IR regime are provided by the following expressions [9, 26-29] (Eq.5)

$$\begin{aligned}
n^2 &= 11.67316 + \frac{1}{\lambda_L^2} + \frac{0.004482633}{\lambda_L^2 - 1.108205^2} && \text{(For Silicon, } 22 \mu\text{m} \geq \lambda_L \geq 2.5 \mu\text{m)} \\
n^2 &= 1 + \frac{10.6684293\lambda_L^2}{\lambda_L^2 - 0.301516485^2} + \frac{0.0030434748\lambda_L^2}{\lambda_L^2 - 1.13475115^2} + \frac{1.54133408\lambda_L^2}{\lambda_L^2 - 1104^2} && \text{(For Silicon, } 2.5\mu\text{m} \geq \lambda_L \geq 1.36 \mu\text{m)} \\
n^2 &= 1 + \frac{0.6961663\lambda_L^2}{\lambda_L^2 - 0.0684043^2} + \frac{0.4079426\lambda_L^2}{\lambda_L^2 - 0.11624142^2} + \frac{0.8974794\lambda_L^2}{\lambda_L^2 - 9.896161^2} && \text{(For Fused Silica)}
\end{aligned} \tag{5}$$

On the other hand, the expression that provides the dynamics of the dielectric function due to the variation of the density of the carriers in an excited material  $N_e^{(a)}$  is given by Eq.6 ( $a=1$  for SiO<sub>2</sub> and  $a=2$  for Si)

$$\varepsilon^{(a)} = 1 + (\varepsilon_{un}^{(a)} - 1) \left( 1 - \frac{N_e^{(a)}}{N_V^{(a)}} \right) \frac{e^2 N_e^{(a)}}{m_r m_e \varepsilon_0 \omega_L^2} \frac{1}{\left( 1 + i \frac{1}{\omega_L \tau_c} \right)} \tag{6}$$

In Eq.6,  $\varepsilon_{un}^{(a)}$  corresponds to the dielectric parameter of the unexcited material that is  $\lambda_L$ -dependent which is calculated from Eq.5,  $N_e^{(a)}$  and  $N_V^{(a)}$  are the carrier densities in the conduction and valence bands ( $N_V^{(1)} = 2.2 \times 10^{22} \text{cm}^{-3}$  [20] and  $N_V^{(2)} = 5 \times 10^{22} \text{cm}^{-3}$  [31], respectively,  $m_e$  is the electron mass,  $e$  is the electron charge,  $m_r = 0.18$ ,  $\varepsilon_0$  is the vacuum permittivity,  $\omega_L$  is the laser frequency and  $\tau_c = 5$  fs stands for the electron collision time. It is recalled that various values for  $\tau_c$  have been used in previous reports (see Ref. [21] and references therein). Furthermore, it is noted that the contribution of Kerr effect for Mid-IR fs pulses in the dielectric function has been taken into account for Si [9] and SiO<sub>2</sub> [21].

Finally, the thermal response of the Si/SiO<sub>2</sub> is described via the employment of the traditional Two-Temperature Model (TTM) for the two materials. In particular, the relaxation-time approximation to Boltzmann's transport equation is used to provide the electron  $T_e^{(Si)}$  and lattice  $T_L^{(Si)}$  temperature, respectively, of Si

$$\begin{aligned}
C_e^{(Si)} \frac{\partial T_e^{(Si)}}{\partial t} &= \frac{\partial}{\partial z} \left( k_e^{(Si)} \frac{\partial T_e^{(Si)}}{\partial z} \right) - G_{cL} (T_e^{(Si)} - T_L^{(Si)}) + S \\
C_L^{(Si)} \frac{\partial T_L^{(Si)}}{\partial t} &= \frac{\partial}{\partial z} \left( k_L^{(Si)} \frac{\partial T_L^{(Si)}}{\partial z} \right) + G_{cL} (T_e^{(Si)} - T_L^{(Si)})
\end{aligned} \tag{7}$$

where  $C_e^{(Si)}$  and  $C_L^{(Si)}$  stand for the heat capacities of the carriers and the lattice, respectively,  $G_{cL}$  is the carrier-phonon coupling,  $k_L^{(Si)}$ , ( $k_e^{(Si)}$ ) correspond to the lattice's (carrier's) thermal conductivity and  $S$  stands for a generalized 'source' term given by the following expression [9]

$$\begin{aligned}
S &= \alpha_{FCA} I + \beta_{TPA} I^2 + \gamma_{TPA} I^3 - \gamma (N_e^{(Si)})^3 - \vec{\nabla} \cdot \vec{W} - \frac{\partial N_e^{(Si)}}{\partial t} (E_g + 3k_B T_e^{(Si)}) - N_e^{(Si)} \left( \frac{\partial E_g}{\partial T_L^{(Si)}} \frac{\partial T_L^{(Si)}}{\partial t} + \frac{\partial E_g}{\partial N_e^{(Si)}} \frac{\partial N_e^{(Si)}}{\partial t} \right) \\
\vec{W} &= (E_g + 4k_B T_e^{(Si)}) \vec{j} - (k_e^{(Si)} + k_h^{(Si)}) \vec{\nabla} T_e^{(Si)} \\
\vec{j} &= D \left( \vec{\nabla} N_e^{(Si)} + \frac{N_e^{(Si)}}{2k_B T_e^{(Si)}} \vec{\nabla} E_g + \frac{N_e^{(Si)}}{2T_e^{(Si)}} \vec{\nabla} T_e^{(Si)} \right)
\end{aligned} \tag{8}$$

where  $E_g$  stands for the energy gap of Silicon,  $k_B$  is the Boltzmann constant,  $D$  is the ambipolar carrier diffusivity.

By contrast, a similar TTM which describes the electron and lattice temperature evolution for fused silica is not used in this work. This is due to the fact simulation predictions demonstrate that no energy absorption occurs in the dielectric material which implies that no electron excitation is produced. Therefore, no noticeable thermal effects are expected and the only but insignificant increase in the latticed temperature of SiO<sub>2</sub> takes place near the interface due to heat transfer from the substrate (see next Section).

### III. SIMULATION PROCEDURE

To solve Eqs.1-8, an iterative Crank-Nicolson scheme is used which is based on a finite-difference method [19]. A small and insignificant variation of the lattice temperature on SiO<sub>2</sub>, mostly, at the back end of the film is calculated through the boundary conditions considered on the interface between the top layer and the substrate:  $k_L \frac{\partial T_L}{\partial z} = k_L^{(Si)} \frac{\partial T_L^{(Si)}}{\partial z}$ , where  $k_L$  stands for the lattice heat conductivity in SiO<sub>2</sub>, respectively, while  $T_L$  corresponds to the lattice temperature in SiO<sub>2</sub>. Finally, it is assumed that there is no carrier diffusion from SiO<sub>2</sub> into Si. Thus, the boundary condition  $\frac{\partial N_e}{\partial z} = \frac{\partial N_e}{\partial z} = 0$  is considered on the interface. Due to the absence of electron excitation in fused silica at all times this boundary condition

turns to:  $\frac{\partial N_e^{(si)}}{\partial z} = 0$  (and  $N_e = 0$ ). It is noted that in this work simulations were performed assuming laser pulses of wavelength  $\lambda_L = 3.2 \mu\text{m}$  and pulse duration  $\tau_p = 170 \text{ fs}$  (unless otherwise stated).

#### IV. RESULTS AND DISCUSSION

Simulations are firstly performed at  $\lambda_L = 3.2 \mu\text{m}$  where the refractive indices of the materials such as air, Si and  $\text{SiO}_2$  are equal to  $\tilde{N}_a = 1$ ,  $\tilde{N}_s = 3.4309$  [32],  $\tilde{N}_m = 1.4143$  [33], respectively (at room temperature). Although the predominant focus of the current work is centred on the investigation of the response of the  $\text{SiO}_2/\text{Si}$  at  $\lambda_L = 3.2 \mu\text{m}$ , a similar exploration can be performed at other laser wavelengths.

Without a loss of generality calculations are performed for  $d$  between 20 nm and 5  $\mu\text{m}$ . Simulation results predict some interesting features of the optical parameters which are illustrated in Fig.2. More specifically, theoretical calculations shown in Fig.2a indicate a dependence of  $R$  and  $T$  on  $d$  which demonstrates that  $R+T=1$ ; this result confirms that no energy is absorbed from  $\text{SiO}_2$  (at 300 K). According to the theoretical predictions (Fig.2a), the range of values of the reflectivity lie between 0.07 and 0.3 while the amount of the energy transmitted into the substrate varies between 0.7 and 0.93 of the deposited energy. These calculations manifest that the antireflection properties of the complex can be controlled by an appropriately selected thickness of the  $\text{SiO}_2$  film. Interestingly, there exists a pronounced periodicity of the optical parameter dependence as a function of thickness demonstrated in Figs.2a,b,d; this is due to the term  $\beta = 2\pi d \tilde{N}_m / \lambda_L$  in the expression that provides the reflectivity and the transmissivity (Eq.1). According to Eq.1,  $\beta$  is included in  $e^{2\beta j}$

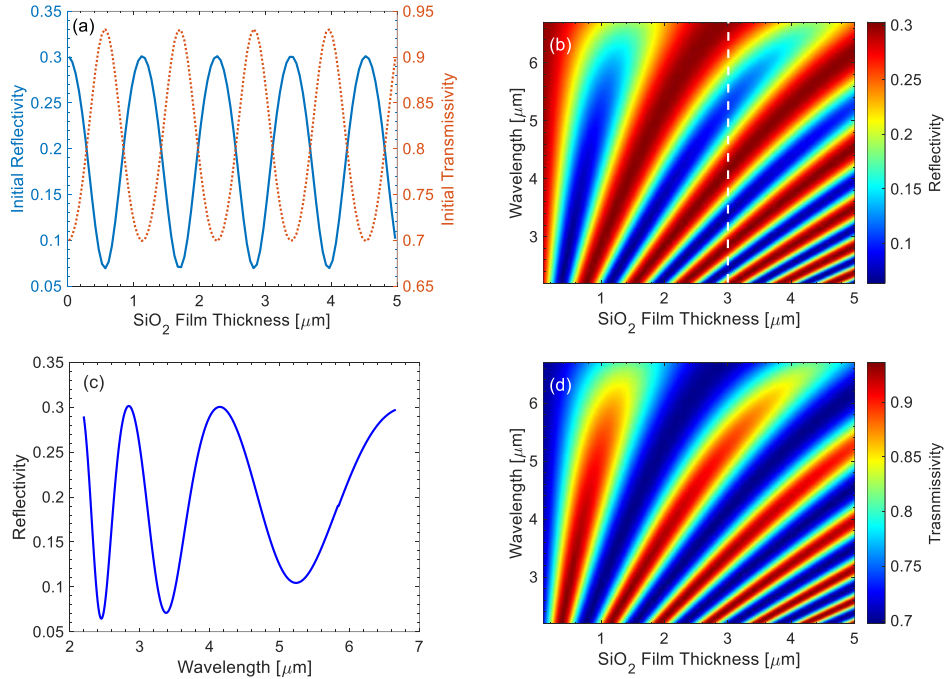


Figure 2: (a) Optical parameters of  $\text{SiO}_2/\text{Si}$  as a function of  $\text{SiO}_2$  thickness (for  $\lambda_L = 3.2 \mu\text{m}$ ), (b) Reflectivity of  $\text{SiO}_2/\text{Si}$  as a function of  $d$  and the laser wavelength, (c) Reflectivity of  $\text{SiO}_2/\text{Si}$  at various wavelengths along the *white* dashed line in (b), at  $d = 3 \mu\text{m}$ , (d) Transmissivity of  $\text{SiO}_2/\text{Si}$  as a function of  $d$  and the laser wavelength. Calculations are at room temperature.

which leads to a (spatially) periodic behaviour of the optical parameters. Thus, the part of the laser energy (at room temperature) is expected to follow a similar trend and, in the next paragraphs, it will be shown that this periodicity will also be projected on the excitation (i.e. carriers) and thermal response (including the damage threshold) of the system. Theoretical results depicted in Fig.2b,c,d indicate that the periodicity at increasing wavelength increases. This is due to the fact that  $\tilde{N}_m$  drops at increasing  $\lambda_L$  which yields a smaller value of  $\beta$  and therefore, a larger periodicity. More specifically, an analysis of the predictions at  $d = 3 \mu\text{m}$  (*white* dashed line in Fig.2b and produced results shown in Fig.2c) confirms the dependence of the reflectivity as increasing wavelength for the same  $\text{SiO}_2$  film thickness. A similar behaviour was also reported in a previous work for a different configuration where a Si film of thickness  $d$  was placed on top of a  $\text{SiO}_2$  substrate [17].

To explore the damage conditions following irradiation of the two-layered complex with Mid-IR fs pulses, it is important to analyse the ultrafast phenomena and derive the induced thermal response of the system. Results in Fig.3

provide the dynamics of the electron density on the surface of the semiconducting material (Fig.3a) and the temporal evolution of  $N_e^{(Si)}$  inside Si (Fig.3b) assuming irradiation of SiO<sub>2</sub>/Si with fluence  $F=0.1$  J/cm<sup>2</sup> considering a SiO<sub>2</sub> film of  $d=520$  nm. Similar results are deduced (results are not shown here) at other  $d$  and  $F$  values for which a  $d$ -dependent maximum electron density is produced as the absorbed energy from SiO<sub>2</sub> varies with  $d$ . It is evident that unlike fused silica, Si absorbs significantly leading to high levels of excitation ( $\sim 1.05 \times 10^{21}$  cm<sup>-3</sup>). The spatiotemporal carrier density distribution inside 1  $\mu$ m of Si within 3 ps is illustrated in Fig.3b. Similarly, the lattice temperature distribution is depicted for the same laser conditions in Fig.3c.

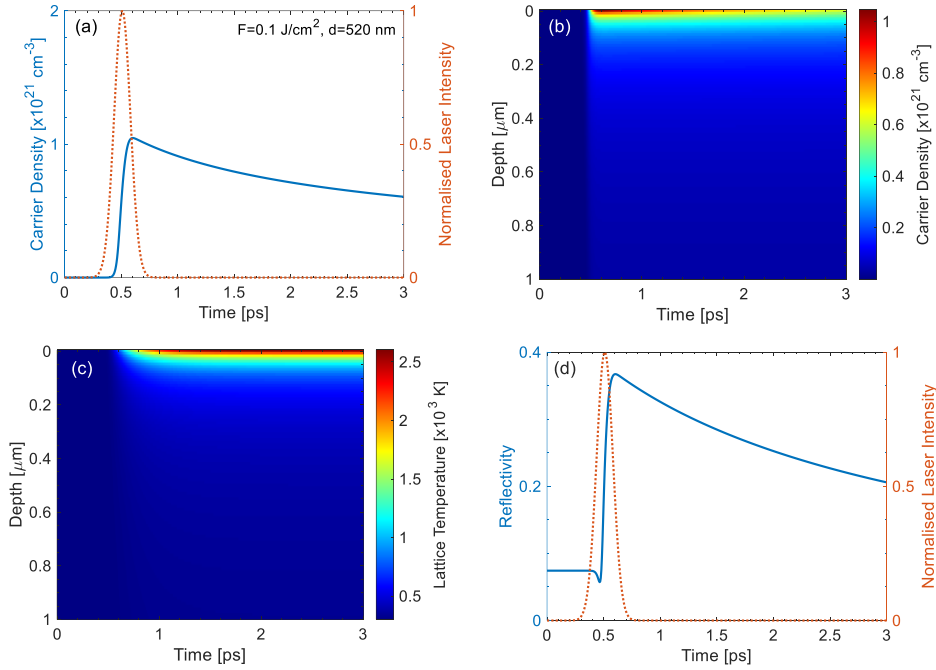


Figure 3: (a) Electron density evolution on the surface of Si. Electron density (b) and Lattice temperature (c) evolution inside Si. (d) Reflectivity dynamics of SiO<sub>2</sub>/Si. ( $F=0.1$  J/cm<sup>2</sup>,  $d=520$  nm).

A key issue that requires a particular investigation is the trend of the optical parameters *during* the pulse. It is noted that results shown in Fig.2 focused on an analysis of the values of  $R$  and  $T$  at room temperature. Nevertheless, a more precise exploration should analyse the fingerprint of the excitation of carriers and ultrafast dynamics on the temporal variation of  $R$  and  $T$ . With respect to the irradiation of semiconducting and dielectric targets with ultrashort laser pulses, it has been demonstrated [9, 30, 31] that the excitation of carriers yields a variation of the dielectric function (Eq.6) and therefore the optical parameters which influence, eventually, the energy absorption from the material (i.e.  $\tilde{N}_S, \tilde{N}_m$  in Eq.1 become a complex number). More specifically, assuming irradiation of the two-layered material with  $F=0.1$  J/cm<sup>2</sup> considering a SiO<sub>2</sub> of  $d=520$  nm, simulation results show there is a

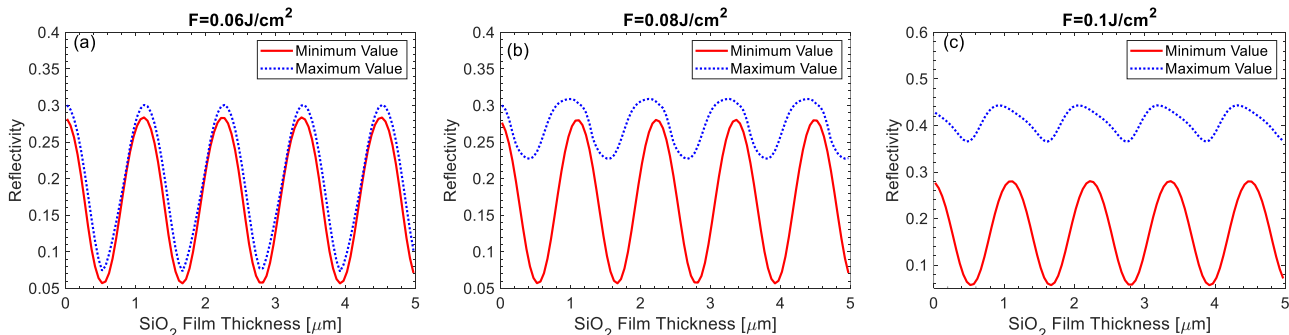


Figure 4: Maximum and Minimum values of Reflectivity of Si/ SiO<sub>2</sub> at various fluences ((a)  $F=0.06$  J/cm<sup>2</sup>, (b)  $F=0.08$  J/cm<sup>2</sup>, (c)  $F=0.1$  J/cm<sup>2</sup>) as a function of the SiO<sub>2</sub> thickness. Simulations are illustrated at  $\lambda_L=3.2$   $\mu$ m.

significant variation of the reflectivity of the complex shown in Fig.3d. The temporal analysis of the optical parameters following the detailed investigation of the ultrafast dynamics show that during the pulse duration the

sum of reflectivity and the transmissivity is equal to one that demonstrates there is no absorption of energy from SiO<sub>2</sub> and therefore  $N_e$  is always zero.

Observing the remarkable variation in the reflectivity during the pulse duration stated in the previous paragraph and before analysing the correlation of the thermal response and the minimum energy required to damage Si with the coating thickness via the employment of fs pulses, it is important to evaluate the levels of the reflected/transmitted amounts of the laser energy derived from the density of excited electrons values. In Fig.4, the minimum and maximum reflectivity values are depicted for  $d$

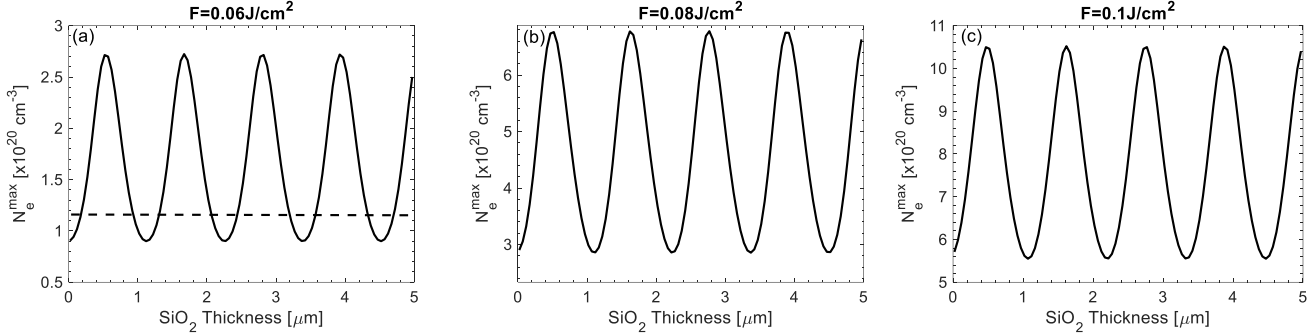


Figure 5: Maximum Carrier density on the Si surface at various fluences ((a)  $F=0.06 \text{ J/cm}^2$ , (b)  $F=0.08 \text{ J/cm}^2$ , (c)  $F=0.1 \text{ J/cm}^2$ ) as a function of the SiO<sub>2</sub> thickness. Simulations are illustrated at  $\lambda_L=3.2 \mu\text{m}$ . Dashed line in (a) indicates OBT.

between 20 nm and 5  $\mu\text{m}$  for  $F=0.06 \text{ J/cm}^2$ ,  $0.08 \text{ J/cm}^2$ ,  $0.1 \text{ J/cm}^2$ . Results show that the reflectivity temporal variation at the lowest fluence is negligible while the increasing excitation at higher fluences leads to an enhanced reflectivity change. Thus, at  $F=0.06 \text{ J/cm}^2$ , there is a rather insignificant variation of  $R$  for some  $d$  while there is a more pronounced change at other SiO<sub>2</sub> thicknesses.

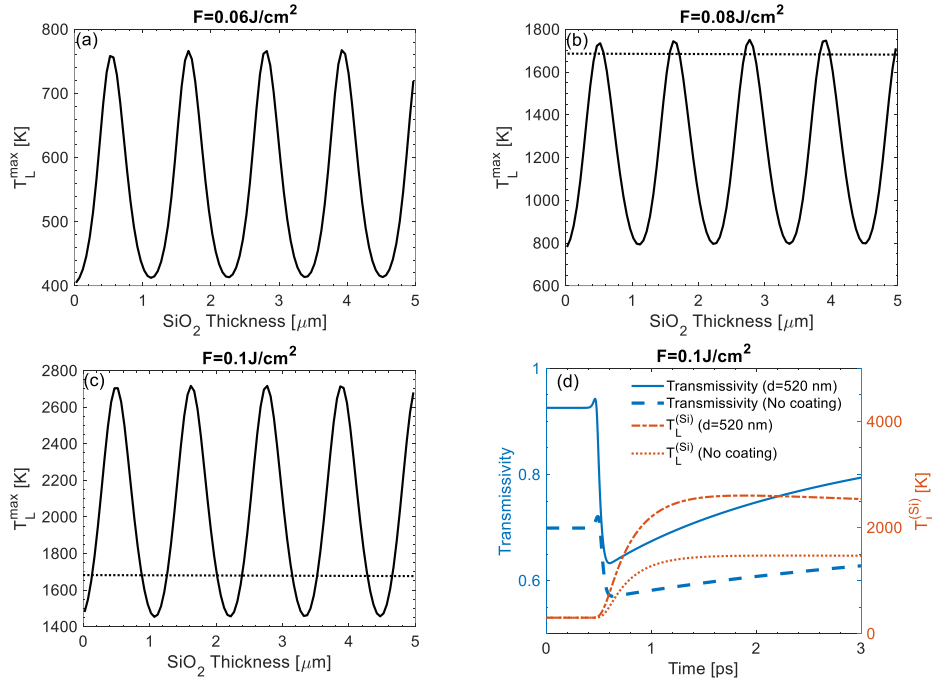


Figure 6: Maximum lattice temperature on the Si surface at various fluences ((a)  $F=0.06 \text{ J/cm}^2$ , (b)  $F=0.08 \text{ J/cm}^2$ , (c)  $F=0.1 \text{ J/cm}^2$ ) as a function of the SiO<sub>2</sub> thickness. Dotted line in (b,c) indicates melting point. (d) Transmissivity in Si for  $d=520 \text{ nm}$  and in absence of SiO<sub>2</sub> ( $F=0.1 \text{ J/cm}^2$ ). Simulations are illustrated at  $\lambda_L=3.2 \mu\text{m}$ .

In addition to the optical parameter variation at different fluences and coating thicknesses, the electron excitation and thermal response of the system are also evaluated. Simulation results illustrated in Fig.5 show a periodic variation of the carrier density as a function of  $d$  for all fluences considered in this work. This is due to the interference effects expressed in the optical parameters (Eq.1) and, therefore, energy absorption  $d$ -dependence. The values of the maximum values of  $N_e^{(Si)}$  (denoted as  $N_e^{\max}$ ) range between  $\sim 10^{20} \text{ cm}^{-3}$  and  $\sim 1.5 \times 10^{21} \text{ cm}^{-3}$ . The black dashed line in Fig.5a corresponds to the critical value  $N_e^{cr}$  (i.e.  $N_e^{cr} \equiv 4\pi^2 c^2 m_e \epsilon_0 / (\lambda_L^2 e^2)$ ) which is, usually, termed as the optical breakdown threshold



(OBT) [23]. In the expression that provides  $N_e^{cr}$ ,  $c$  is the speed of light,  $m_e$  stands for mass of electron,  $e$  is the electron charge and  $\epsilon_0$  is the permittivity of vacuum. In particular,  $N_e^{cr} = 1.09 \times 10^{20} \text{ cm}^{-3}$  at  $\lambda_L = 3.2 \mu\text{m}$ . In previous reports, and more specifically, for dielectrics [25, 34–37], the OBT has been associated with the minimum critical density that leads to material damage and it was, therefore, linked with DT of transparent materials. By contrast, in other works [20, 22, 38, 39], a more precise evaluation of DT was derived via a thermal criterion (i.e. fluence at which the material starts to melt). To evaluate whether the two criteria are similar, the thermal response of the system is calculated. Results at the same fluences as before (Fig.6a,b,c), demonstrate, again, a periodic dependence of the maximum lattice temperature  $T_L^{(Si)}$  (denoted as  $T_L^{max}$ ), however, the melting point (associated directly with DT) is reached in different conditions (black dotted line Fig.6b,c). Thus, a comparison of Figs.5,6 show that the OBT-based threshold provides an underestimation of the DT. According to Fig.6b,  $F=0.08 \text{ J/cm}^2$  represents a fluence value at which the material starts to melt at particular values of  $d$  characterized by a periodicity.

To evaluate the influence of the coating on both the optical response of the complex and the thermal effects on the substrate, simulation results are illustrated in Fig.6d for two cases, where the evolution of the lattice temperature and transmissivity in the Si material are shown: (a) assuming the presence of a  $\text{SiO}_2$  film of thickness  $d=520 \text{ nm}$  and (b) in absence of the fused silica coating. Interestingly, results indicate that for this particular  $\text{SiO}_2$  thickness, the transmissivity increases leading to a larger energy absorption from the substrate which is reflected on a produced larger maximum temperature. Similar conclusions can be deduced for other values of  $d$ , however, as it will be shown in the next section, in contrast to results produced for a different two-layered material (i.e.  $\text{Si/SiO}_2$  which was explored in a previous report [17]) the coating enhances the lattice temperature with direct implications for DT.

While the aforementioned analysis was performed in laser conditions assuming the same photon energy and pulse duration, an evaluation of the ultrafast dynamics and thermal response of the system at different laser wavelengths and pulse duration are expected allow the determination of the impact of those parameters on the physical processes.

### a. Dependence of $N_e^{max}$ , $T_L^{max}$ and DT on the pulse duration

In Fig.7a, the maximum density of the excited carriers on Si,  $N_e^{max}$ , as a function of the coating thickness at three different values of the pulse duration (i.e.  $\tau_p=170 \text{ fs}$ ,  $500 \text{ fs}$ ,  $1 \text{ ps}$ ) at  $\lambda_L = 3.2 \mu\text{m}$  and at  $F=0.1 \text{ J/cm}^2$  are illustrated. Due to the fact that longer pulse durations yield smaller energy deposition and, eventually, energy absorption from Si, the maximum carrier density is expected to drop at increasing  $\tau_p$  for the same  $d$ . A similar trend is revealed for the maximum lattice temperature  $T_L^{max}$  (Fig.7b). As expected, both parameters exhibit a periodic dependence on the  $\text{SiO}_2$  thickness. Finally, for the three pulse durations, DT as a function of  $d$  is illustrated in Fig.7c. The horizontal *dotted* lines correspond to the DT of Si,  $F_{\tau_p}^{(Si)}$ , following irradiation with  $\tau_p=170 \text{ fs}$ ,  $500 \text{ fs}$ ,  $1 \text{ ps}$ , respectively, in *absence* of the  $\text{SiO}_2$  coating (i.e.  $F_{\tau_p=170 \text{ fs}}^{(Si)} = 0.11 \text{ J/cm}^2$ ,  $F_{\tau_p=500 \text{ fs}}^{(Si)} \sim 0.18 \text{ J/cm}^2$ ,  $F_{\tau_p=1 \text{ ps}}^{(Si)} \sim 0.25 \text{ J/cm}^2$ ). As expected,  $F_{\tau_p}^{(Si)}$  exhibit an increasing trend at increasing pulse temporal width. Simulation results in Fig.7c manifest a noticeable variation of DT with  $d$ . For all three

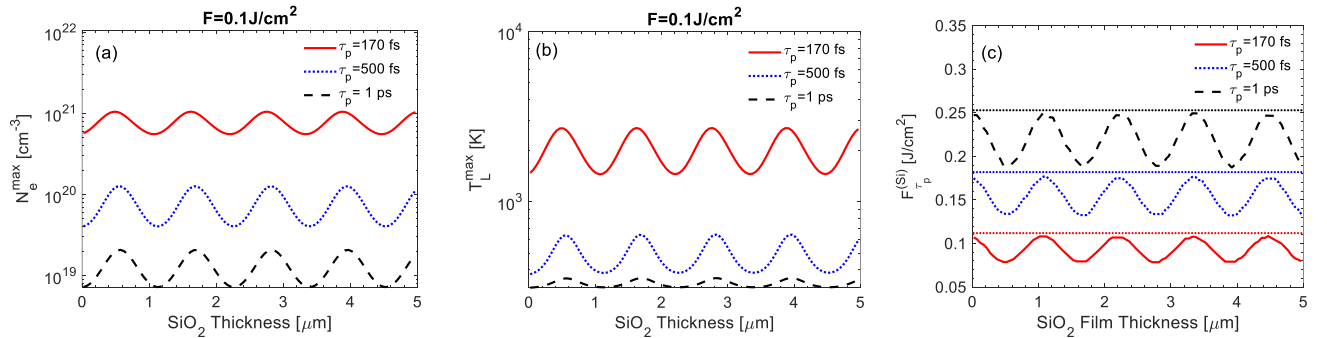


Figure 7: Maximum Carrier density (a) and lattice temperature (b) on the Si surface ( $F=0.1 \text{ J/cm}^2$ ) and (c) damage threshold calculation as a function of the  $\text{SiO}_2$  thickness at various pulse durations ( $\tau_p=170 \text{ fs}$ ,  $500 \text{ fs}$ ,  $1 \text{ ps}$ ). Horizontal *dotted* lines above the curves in (c) correspond to DT of Si in absence of the coating for corresponding  $\tau_p$ . Simulations are illustrated at  $\lambda_L=3.2 \mu\text{m}$ .

values of the pulse duration considered in this work, in principle, there is a *decrease* of DT with a respect to the case in which the fused silica coating is absent. An analysis of the results illustrated in Fig.7c show a significant drop by 27% of DT can be achieved if coating is placed on the substrate. Furthermore, the variation of DT with the coating thickness can reach 25% for the three pulse durations which emphasises the role of the distinct ultrafast phenomena at different excitation conditions.

Unlike predictions reported in a previous work (i.e. for a  $\text{Si/SiO}_2$  [17]), the presence of the coating leads to a *drop* of the threshold for inducing damage on the substrate. This can be attributed to the different optical properties of the



complex due to the placement of a lower refractive index material on the Si substrate which leads to an enhanced energy absorption from the substrate (Fig.6d). Interestingly, for all three pulse durations in this investigation, the maximum carrier density produced on Si is higher than the OBT,  $N_e^{cr}$ . More specifically,  $N_e^{max}$  for  $\tau_p=170$  fs, 500 fs, 1 ps are calculated to be equal to  $N_e^{max} \sim 6.5 \times 10^{20} \text{ cm}^{-3}$ ,  $3.8 \times 10^{20} \text{ cm}^{-3}$ ,  $2.8 \times 10^{20} \text{ cm}^{-3}$ , respectively. These results serve as a justification that the determination of DT via a thermal criterion constitutes a more accurate methodology than the OBT; results, also, confirm that the OBT-based evaluation of the DT presents a necessary but not sufficient condition for the onset of damage.

## b. Dependence of $N_e^{max}$ , $T_L^{max}$ and DT on the laser wavelength

To evaluate the influence of the laser photon energy on the ultrafast dynamics and thermal response of the two-layered complex, a detailed analysis was performed of the maximum density of the excited carriers on Si as a function of the coating thickness at three different laser wavelengths (i.e.  $\lambda_L = 2.2 \mu\text{m}$ ,  $2.6 \mu\text{m}$ ,  $3.2 \mu\text{m}$ ) at  $\tau_p=170$  fs and at  $F=0.1 \text{ J/cm}^2$ . Results are illustrated in Fig.8a. As explained above, the increase of the periodicity of the optical parameters demonstrated at increasing laser wavelength (Fig.2b,c,d) is also exhibited by the absorbed energy, the carrier density (Fig.8a) and lattice temperature (Fig.8b), also, exhibit a similar trend. Finally, for the three laser wavelengths, DT as a function of  $d$  is illustrated in Fig.8c.

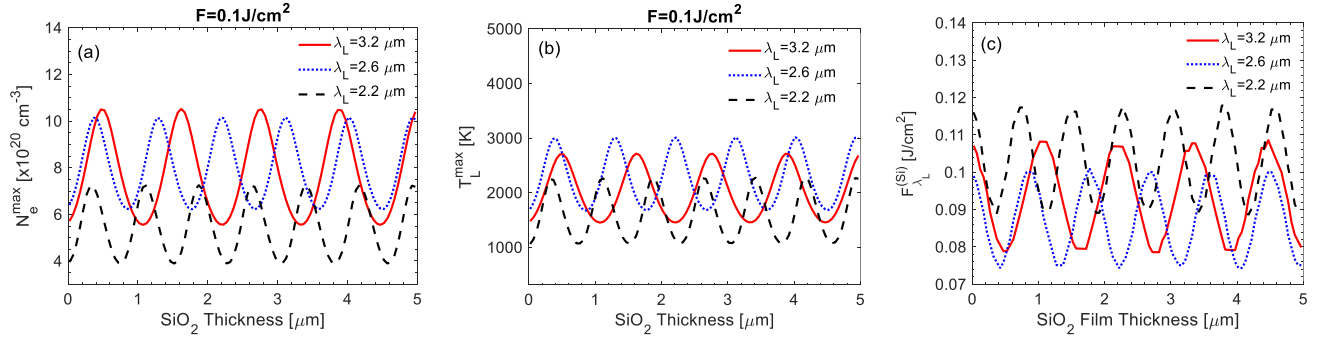


Figure 8: Maximum Carrier density (a) and maximum Carrier lattice temperature (b) on the Si surface ( $F=0.1 \text{ J/cm}^2$ ) and (c) damage threshold as a function of the SiO<sub>2</sub> thickness at various laser wavelength ( $\lambda_L=2.2 \mu\text{m}$ ,  $2.6 \mu\text{m}$ ,  $3.2 \mu\text{m}$ ). Simulations are illustrated at  $\tau_p=170$  fs.

To elaborate further on the dependence of the magnitude of the  $N_e^{max}$ ,  $T_L^{max}$  on the coating thickness at various laser wavelengths, it is important to correlate the dominant processes and the magnitude of the absorbed energy from the substrate. The remarkable smaller  $N_e^{max}$ ,  $T_L^{max}$  at the shortest laser wavelength ( $\lambda_L = 2.2 \mu\text{m}$ ) for the same  $d$  might be confusing as a larger photon energy is possibly expected to facilitate the electron excitation leading to a smaller DT. A conclusive interpretation of the results and the behaviour of  $N_e^{max}$ ,  $T_L^{max}$  with respect to the laser wavelength and  $d$  requires a detailed analysis of: (a) the energy absorbed from the substrate for the same SiO<sub>2</sub> thickness at different wavelength and (b) the evaluation of other processes which can be more efficient in the production of excited carriers than the multiphoton ionization.

To evaluate the role of the latter, simulations conducted for three representative values of the coating thickness (similar results can be derived for other  $d$ )  $d=20$  nm, 720 nm and 1220 nm at  $\lambda_L = 2.2 \mu\text{m}$ ,  $2.6 \mu\text{m}$ ,  $3.2 \mu\text{m}$  for  $0.1 \text{ J/cm}^2$  showed that the impact ionization does not account for this behavior. More specifically, an analysis of the contribution of the impact ionization process manifests that the inclusion of this ionisation mechanism simply increases the carrier density as expected; it does not alter, though, the wavelength-dependent carrier density order at any coating thickness (see Supplementary Material). By contrast, results of the transmissivity evolution for the three values of thickness and at  $\lambda_L = 2.2 \mu\text{m}$ ,  $2.6 \mu\text{m}$ ,  $3.2 \mu\text{m}$  for  $0.1 \text{ J/cm}^2$  (see Supplementary Material) show that the monotonicity of  $N_e^{max}$  and evolution of  $N_e^{(Si)}$  are attributed to the amount of energy absorbed from the material. Analysing the monotonicity of the carrier density curves for the three representative (but of distinct interest due optical parameter behaviour) thicknesses, it is noted that:

- (i) For  $d=20$  nm, the absorbed energy from Si is *almost* identical for all three wavelengths at room temperature. When the pulse is switched on and till almost the maximum of the laser energy (i.e. peak of the laser intensity), the absorbed energy will be the largest for  $\lambda_L = 2.6 \mu\text{m}$  followed by that for  $\lambda_L = 2.2 \mu\text{m}$ ; by contrast, at longer times the absorbed energy for  $\lambda_L = 2.2 \mu\text{m}$  will dominate. This behaviour will be projected on the  $N_e^{max}$  (Fig.8a).
- (ii) For  $d=720$  nm, the absorbed energy from Si is *not* identical for the three wavelengths at room temperature. More specifically, the transmissivity is larger for  $\lambda_L = 3.2 \mu\text{m}$  followed by that for  $\lambda_L = 2.6 \mu\text{m}$  and then

for  $\lambda_L = 2.2 \mu\text{m}$ . When the pulse is switched on and till almost the maximum of the laser energy (i.e. peak of the laser intensity), this monotonicity is preserved resulting into the aforementioned behaviour being projected on the  $N_e^{max}$  (Fig.8a).

- (iii) For  $d=1220 \text{ nm}$ , the absorbed energy from Si is *not* again identical for the three wavelengths at room temperature. More specifically, the transmissivity for  $\lambda_L = 2.2 \mu\text{m}$  is a little larger than the transmissivity for  $\lambda_L = 2.6 \mu\text{m}$  but significantly larger than that of  $\lambda_L = 3.2 \mu\text{m}$  (at room temperature). When the pulse is switched on, the first laser wavelength will lead to a very small increase in the absorption level compared to the case before the application of the pulse. By contrast, the second wavelength ( $\lambda_L = 2.6 \mu\text{m}$ ) which has not a very significantly different initial transmissivity from that of  $\lambda_L = 2.2 \mu\text{m}$  will lead to an increase of the absorption level (Fig.8a). Thus, the produced  $N_e^{max}$  for  $\lambda_L = 2.6 \mu\text{m}$  will be higher than that of  $\lambda_L = 2.2 \mu\text{m}$ . Finally, the third wavelength ( $\lambda_L = 3.2 \mu\text{m}$ ) that yields a significantly smaller transmissivity gives  $N_e^{max}$  smaller than the other two wavelengths.

To summarise, the theoretical predictions presented in this work manifest that a modulation of the optical parameters, ultrafast dynamics and damage threshold are possible through an appropriate selection of the thickness of  $\text{SiO}_2$ . Interesting physical phenomena and dependencies appear to occur at various laser wavelengths and pulse durations assuming different thicknesses of the coating. The development of appropriate experimental protocols is certainly required to validate the theoretical model. Further investigation in different conditions such as shorter pulse durations or longer laser wavelengths will allow to attain a more complete picture of the underlying physical mechanisms occurring following irradiation of multi-layered materials with Mid-IR fs pulses. Nevertheless, the methodology presented in this work is aimed to provide a first and comprehensive insight into the physical processes that describe irradiation of two-layered materials (both transparent in this spectral region) with femtosecond mid-IR laser pulses. In addition to an interest from a fundamental point of view, elucidation of the physical phenomena occurring in this spectral regime is expected to allow a systematic novel surface engineering with strong mid-IR fields.

## V. CONCLUSIONS

In this work, a detailed analysis of the ultrafast phenomena and thermal response of a  $\text{SiO}_2$  coating on Si of various thicknesses of the coating following irradiation of the complex with ultrashort pulsed lasers in the Mid-IR range was presented. Results demonstrated a periodic variation of the optical parameters with the thickness of  $\text{SiO}_2$  derived via the employment of multireflection theory and taking into account interference processes. It was shown that the periodic behavior was projected into the ultrafast dynamics of the excited carriers and thermal response of the substrate while no part of laser energy is absorbed from the coating itself. A remarkable impact of the coating thickness was manifested and it can be used to modulate the damage threshold of Si while it was shown that this parameter can decrease the threshold by up to 27% in comparison to the value in absence of the coating. Similar conclusions were deduced for various fluences, pulse durations and laser wavelengths while the pronounced role of the absorbed energy from the substrate on the damage threshold was emphasised. The elucidation of the laser driven physical phenomena that characterize the response of optical coatings on materials with Mid-IR fs pulses via this analysis and the remarkable predictions can be employed for the development of new tools for nonlinear optics and photonics for a large range of Mid-IR laser-based applications.

## ACKNOWLEDGEMENTS

The authors would like to acknowledge financial support from *HELLAS-CH* project (MIS 5002735), implemented under the “Action for Strengthening Research and Innovation Infrastructures” funded by the Operational Programme “Competitiveness, Entrepreneurship and Innovation” and co-financed by Greece and the EU (European Regional Development Fund).

Corresponding authors:

\* George D.Tsibidis: [tsibidis@iesl.forth.gr](mailto:tsibidis@iesl.forth.gr) (Theory and Simulations)

♦ Emmanuel Stratakis: [stratak@iesl.forth.gr](mailto:stratak@iesl.forth.gr)

## REFERENCES

- [1] M. Ebrahim-Zadeh, G. Leo, I. Sorokina, Mid-Infrared Coherent Sources and Applications: introduction, *J. Opt. Soc. Am. B*, 35 (2018) MIC1-MIC1.
- [2] B. Jalali, SILICON PHOTONICS Nonlinear optics in the mid-infrared, *Nat Photonics*, 4 (2010) 506-508.
- [3] H. Pires, M. Baudisch, D. Sanchez, M. Hemmer, J. Biegert, Ultrashort pulse generation in the mid-IR, *Progress in Quantum Electronics*, 43 (2015) 1-30.
- [4] R. Soref, Mid-infrared photonics in silicon and germanium, *Nat Photonics*, 4 (2010) 495-497.
- [5] R. Stanley, Plasmonics in the mid-infrared, *Nat Photonics*, 6 (2012) 409-411.
- [6] A. Ramer, O. Osmani, B. Rethfeld, Laser damage in silicon: Energy absorption, relaxation, and transport, *Journal of Applied Physics*, 116 (2014) 053508.
- [7] G.D. Tsibidis, M. Barberoglou, P.A. Loukakos, E. Stratakis, C. Fotakis, Dynamics of ripple formation on silicon surfaces by ultrashort laser pulses in subablation conditions, *Physical Review B*, 86 (2012) 115316.
- [8] P.P. Pronko, P.A. VanRompay, C. Horvath, F. Loesel, T. Juhasz, X. Liu, G. Mourou, Avalanche ionization and dielectric breakdown in silicon with ultrafast laser pulses, *Physical Review B*, 58 (1998) 2387-2390.
- [9] E. Petrakakis, G.D. Tsibidis, E. Stratakis, Modelling of the ultrafast dynamics and surface plasmon properties of silicon upon irradiation with mid-IR femtosecond laser pulses, *Physical Review B*, 99 (2019) 195201.
- [10] M.R. Shcherbakov, K. Werner, Z. Fan, N. Talisa, E. Chowdhury, G. Shvets, Photon acceleration and tunable broadband harmonics generation in nonlinear time-dependent metasurfaces, *Nat Commun*, 10 (2019) 1345.
- [11] K. Werner, V. Gruzdev, N. Talisa, K. Kafka, D. Austin, C.M. Liebig, E. Chowdhury, Single-Shot Multi-Stage Damage and Ablation of Silicon by Femtosecond Mid-infrared Laser Pulses, *Sci Rep-Uk*, 9 (2019) 19993.
- [12] S. Maragkaki, G.D. Tsibidis, L. Haizer, Z. Papa, R. Flender, B. Kiss, Z. Marton, E. Stratakis, Tailoring surface topographies on solids with Mid-IR femtosecond laser pulses, *Applied Surface Science*, 612 (2023) 155879.
- [13] K. Werner, E. Chowdhury, Extreme Sub-Wavelength Structure Formation from Mid-IR Femtosecond Laser Interaction with Silicon, *Nanomaterials-Basel*, 11 (2021) 1192.
- [14] D.R. Austin, K.R.P. Kafka, Y.H. Lai, Z. Wang, K.K. Zhang, H. Li, C.I. Blaga, A.Y. Yi, L.F. DiMauro, E.A. Chowdhury, High spatial frequency laser induced periodic surface structure formation in germanium by mid-IR femtosecond pulses, *Journal of Applied Physics*, 120 (2016) 143103.
- [15] J. Amirloo, S.S. Saini, M. Dagenais, Comprehensive study of antireflection coatings for mid-infrared lasers, *J Vac Sci Technol A*, 34 (2016) 061505.
- [16] M. Zinoviev, N.N. Yudin, S. Podzvalov, E. Slyunko, N.A. Yudin, M. Kulesh, I. Dorofeev, H. Baalbaki, Optical AR Coatings of the Mid-IR Band for ZnGeP<sub>2</sub> Single Crystals Based on ZnS and Oxide Aluminum, *Crystals*, 12 (2022) 1169.
- [17] G.D. Tsibidis, E. Stratakis, Influence of antireflection Si coatings on the damage threshold of fused silica upon irradiation with mid-IR femtosecond laser pulses, *Optics Letters*, 48 (2023) 4841-4844.
- [18] M. Born, E. Wolf, Principles of optics : electromagnetic theory of propagation, interference and diffraction of light, 7th expanded ed., Cambridge University Press, Cambridge ; New York, 1999.
- [19] G. Tsibidis, D. Mansour, E. Stratakis, Damage Threshold evaluation for thin metal targets exposed to femtosecond laser pulses: the role of material thickness, *Optics & Laser Technology*, 156 (2022) 108484.
- [20] B. Chimier, O. Uteza, N. Sanner, M. Sentis, T. Itina, P. Lassonde, F. Legare, F. Vidal, J.C. Kieffer, Damage and ablation thresholds of fused-silica in femtosecond regime, *Physical Review B*, 84 (2011) 094104.

- [21] G.D. Tsibidis, E. Stratakis, Ionisation processes and laser induced periodic surface structures in dielectrics with mid-infrared femtosecond laser pulses, *Sci Rep-Uk*, 10 (2020) 8675.
- [22] I. Mirza, N.M. Bulgakova, J. Tomastik, V. Michalek, O. Haderka, L. Fekete, T. Mocek, Ultrashort pulse laser ablation of dielectrics: Thresholds, mechanisms, role of breakdown, *Sci Rep-Uk*, 6 (2016).
- [23] T.E. Itina, N. Shcheblanov, Electronic excitation in femtosecond laser interactions with wide-band-gap materials, *Applied Physics A*, 98 (2010) 769-775.
- [24] B. Rethfeld, Unified model for the free-electron avalanche in laser-irradiated dielectrics, *Physical Review Letters*, 92 (2004) 187401.
- [25] G.D. Tsibidis, E. Stratakis, Ionization dynamics and damage conditions in fused silica irradiated with mid-infrared femtosecond pulses, *Applied Physics Letters*, 122 (2023) 043501.
- [26] N.K. Hon, R. Soref, B. Jalali, The third-order nonlinear optical coefficients of Si, Ge, and Si<sub>1-x</sub>Ge<sub>x</sub> in the midwave and longwave infrared, *Journal of Applied Physics*, 110 (2011) 011301.
- [27] A.D. Bristow, N. Rotenberg, H.M. van Driel, Two-photon absorption and Kerr coefficients of silicon for 850-2200 nm, *Applied Physics Letters*, 90 (2007) 191104.
- [28] Q. Lin, J. Zhang, G. Piredda, R.W. Boyd, P.M. Fauchet, G.P. Agrawal, Dispersion of silicon nonlinearities in the near infrared region, *Applied Physics Letters*, 91 (2007) 021111.
- [29] S. Pearl, N. Rotenberg, H.M. van Driel, Three photon absorption in silicon for 2300-3300 nm, *Applied Physics Letters*, 93 (2008) 131102.
- [30] G.D. Tsibidis, The influence of dynamical change of optical properties on the thermomechanical response and damage threshold of noble metals under femtosecond laser irradiation, *Journal of Applied Physics*, 123 (2018) 085903.
- [31] K. Sokolowski-Tinten, D. von der Linde, Generation of dense electron-hole plasmas in silicon, *Physical Review B*, 61 (2000) 2643-2650.
- [32] D. Chandler-Horowitz, P.M. Amirtharaj, High-accuracy, *Journal of Applied Physics*, 97 (2005) 123526.
- [33] I.H. Malitson, Interspecimen Comparison of Refractive Index of Fused Silica, *Journal of the Optical Society of America*, 55 (1965) 1205-&.
- [34] S. Tzortzakis, B. Lamouroux, A. Chiron, S.D. Moustazis, D. Anglos, M. Franco, B. Prade, A. Mysyrowicz, Femtosecond and picosecond ultraviolet laser filaments in air: experiments and simulations, *Optics Communications*, 197 (2001) 131-143.
- [35] B.C. Stuart, M.D. Feit, S. Herman, A.M. Rubenchik, B.W. Shore, M.D. Perry, Nanosecond-to-femtosecond laser-induced breakdown in dielectrics, *Physical Review B*, 53 (1996) 1749-1761.
- [36] A.C. Tien, S. Backus, H. Kapteyn, M. Murnane, G. Mourou, Short-pulse laser damage in transparent materials as a function of pulse duration, *Physical Review Letters*, 82 (1999) 3883-3886.
- [37] M. Lenzner, Femtosecond laser-induced damage of dielectrics, *Int J Mod Phys B*, 13 (1999) 1559-1578.
- [38] T.Q. Jia, R.X. Li, Z. Liu, Z.Z. Xu, Threshold of femtosecond laser-induced damage in transparent materials, *Applied Physics a-Materials Science & Processing*, 74 (2002) 503-507.
- [39] G.D. Tsibidis, E. Skoulas, A. Papadopoulos, E. Stratakis, Convection roll-driven generation of supra-wavelength periodic surface structures on dielectrics upon irradiation with femtosecond pulsed lasers, *Physical Review B*, 94 (2016) 081305(R).